Rabi sideband narrowing via strongly driven resonance fluorescence in a narrow-bandwidth squeezed vacuum

A. S. Parkins
Department of Physics, University of Waikato, Hamilton, New Zealand
(Received 16 March 1990)

We examine resonance fluorescence of a two-level atom in a squeezed vacuum, under the condition that the squeezing bandwidth is much narrower than the Rabi splitting of the Mollow triplet. For a suitable choice of the relative phase between the squeezed vacuum and coherent driving field, we find significant narrowing of the Rabi peaks and inhibited population decay. These results are in marked contrast to previous broadband squeezing analyses, which predict strong broadening of the Rabi peaks and enhanced population decay. We explore the connection between our work and that on the dynamical suppression of spontaneous emission via strongly driven resonance fluorescence in a cavity [Lewenstein, Mossberg, and Glauber, Phys. Rev. Lett. **59**, 775 (1987)]. By modifying this work to incorporate squeezing of the cavity modes, we are able to combine the features of both systems, and thereby predict strong inhibition of the decay of all three components of the Bloch vector in a possible experimental configuration.

I. INTRODUCTION

In the field of atomic spectroscopy, the introduction of squeezed light to a number of classic problems has led to predictions of novel and interesting phenomena.[1-6] The most dramatic of these has been the prediction of line narrowing in the fluorescence spectrum of a two-level atom. This was first expounded in the context of spontaneous emission in a broadband squeezed vacuum,[1] where it was shown that the two quadratures of the atomic polarization are damped at different rates, one at an enhanced rate and the other at a reduced rate compared to the normal radiative decay of the atom.

With the addition of a coherent driving field, the familiar Mollow triplet was found to exhibit a striking dependence on the relative phases of the squeezed vacuum and the coherent driving field.[2] In particular, the central peak of the triplet could display a subnatural or supernatural linewidth depending on the phase of the driving field. However, the Rabi sidebands could only be broadened relative to their normal vacuum width. These results were again computed in the broadband limit, that is, the bandwidth of squeezed light was assumed to be sufficiently large so as to allow a squeezed white-noise formulation[7] of the problem. This requires the squeezing bandwidth to extend well beyond the Rabi splitting in the fluorescence spectrum (so that the squeezed vacuum appears δ correlated even on the time scale of the Rabi oscillations).

Squeezed white noise is, of course, an idealization. Indeed, present squeezed-light sources (most notably the degenerate parametric amplifier[8]) exhibit bandwidths only of the order of typical atomic linewidths. The effect of finite bandwidth squeezing on spontaneous emission and atomic absorption spectra has been analyzed in detail,[9,10] with the overall conclusion that line-narrowing effects are degraded, and eventually cease to occur, as the squeezing bandwidth is reduced.

The spectrum of resonance fluorescence under finite-bandwidth conditions has not, to our knowledge, been investigated in such detail. Here we shall demonstrate that a finite squeezing bandwidth is not necessarily a disadvantage. After formulating our model in Sec. II, we show in Sec. III that interesting new features are revealed in the fluorescence spectrum in the case where the squeezing bandwidth, though possibly broad compared to the natural atomic linewidths, falls well within the Rabi splitting of the Mollow triplet. In particular, the Rabi sidebands may now be significantly narrowed, and the population decay inhibited, depending on the phase of the driving field. These effects result from a driving-field-induced decoupling that occurs between the narrow bandwidth component of the noisy input field quadrature and the atomic system operators.

Our results can be related to recent work on dynamical modifications of spontaneous emission via strongly driven resonance fluorescence in a cavity.[11] In this case, the cavity spectral density facilitates a vacuum reservoir with finite bandwidth noise properties. In Sec. IV, we modify this earlier work to incorporate squeezing, yielding a model that closely parallels that of Sec. II. In doing so, we find it possible to enhance some of the effects seen in the previous work, while demonstrating our own findings in a possible experimental configuration.

II. MODEL

A. Quantum Langevin equations and the adjoint equation

The approach we shall adopt in treating this problem has been described in some detail in Ref. 9, so for further details the reader is referred to that work. The dynamics of our two-level atom are completely described by the equations of motion for the atomic "spin" operators S^+, S^-, S_z (which can be represented as combinations of the 2×2 Pauli matrices). The quantum Langevin equations

for the operators S^+ and S_z have the form

$$\begin{aligned}\dot{S}^+ &= i\omega_a S^+ - i\Omega_0 \cos(\omega_0 t-\phi_0) S_z \\ &\quad -\frac{i}{2}\left[\frac{\gamma_a}{\hbar\omega_a}\right]^{1/2}[E_{\text{in}}(t),S_z]_+ , \\ \dot{S}_z &= -\gamma_a - 2i\Omega_0\cos(\omega_0 t-\phi_0)(S^+-S^-) \\ &\quad -i\left[\frac{\gamma_a}{\hbar\omega_a}\right]^{1/2}[E_{\text{in}}(t),S^+-S^-]_+ ,\end{aligned} \tag{2.1}$$

where ω_a is the atomic transition frequency, γ_a is the natural linewidth of the transition, and Ω_0 and ϕ_0 are the Rabi frequency and phase, respectively, of the coherent driving field. The incoming electric field operator $E_{\text{in}}(t)$ (representing the incoherent portion of the field) is evaluated at the position of the atom, and may be expressed in terms of quadrature phase operators as

$$E_{\text{in}}(t)=E_1(t)\cos(\omega_0 t)+E_2(t)\sin(\omega_0 t) , \tag{2.2}$$

where ω_0 is the frequency of the coherent driving field.

We move to a frame rotating at frequency ω_0, and define polarization quadratures that are in phase and out of phase with the coherent driving field,

$$\begin{aligned}S_x &= S^+ e^{-i\omega_0 t+i\phi_0}+S^- e^{i\omega_0 t-i\phi_0} , \\ S_y &= -i(S^+ e^{-i\omega_0 t+i\phi_0}-S^- e^{i\omega_0-i\phi_0}) .\end{aligned} \tag{2.3}$$

With rapidly rotating terms removed (rotating wave approximation), the equations of motion become

$$\begin{aligned}\dot{S}_x &= -\Delta_a S_y+\frac{1}{2}\left[\frac{\gamma_a}{\hbar\omega_a}\right]^{1/2}[E_1(t)\sin(\phi_0)-E_2(t)\cos(\phi_0),S_z]_+ , \\ \dot{S}_y &= \Delta_a S_x-\Omega_0 S_z-\frac{1}{2}\left[\frac{\gamma_a}{\hbar\omega_a}\right]^{1/2}[E_1(t)\cos(\phi_0)+E_2(t)\sin(\phi_0),S_z]_+ , \\ \dot{S}_z &= -\gamma_a+\Omega_0 S_y+\frac{1}{2}\left[\frac{\gamma_a}{\hbar\omega_a}\right]^{1/2}[E_1(t)\cos(\phi_0)+E_2(t)\sin(\phi_0),S_y]_+ -\frac{1}{2}\left[\frac{\gamma_a}{\hbar\omega_a}\right]^{1/2}[E_1(t)\sin(\phi_0)-E_2(t)\cos(\phi_0),S_x]_+ ,\end{aligned} \tag{2.4}$$

where $\Delta_a=\omega_a-\omega_0$. Following Ref. 9, we develop from these equations an adjoint equation for a quantity $\mu(t)$ which is 2×2 matrix functional of the incoming electric field operator $E_{\text{in}}(t)$. Defining

$$\bar{S}_i(t)\equiv \text{Tr}_{\text{sys}}[S_i\mu(t)] \tag{2.5}$$

as the *atomic* average of the spin operators, we derive the following equations:

$$\begin{aligned}\dot{\bar{S}}_x &= -\Delta_a\bar{S}_y-\beta_X(t)\bar{S}_z , \\ \dot{\bar{S}}_y &= \Delta_a\bar{S}_x-\Omega_0\bar{S}_z-\beta_Y(t)\bar{S}_z , \\ \dot{\bar{S}}_z &= -\gamma_a+\Omega_0\bar{S}_y+\beta_X(t)\bar{S}_x+\beta_Y(t)\bar{S}_y ,\end{aligned} \tag{2.6}$$

where $\beta_X(t)$ and $\beta_Y(t)$ are defined by

$$\begin{aligned}\beta_X(t)\rho &= \frac{1}{2}\left[\frac{\gamma_a}{\hbar\omega_a}\right]^{1/2}\{-\sin(\phi_0)[E_1(t),\rho]_+ \\ &\quad +\cos(\phi_0)[E_2(t),\rho]_+\} \\ &\equiv[-\sin(\phi_0)\beta_1(t)+\cos(\phi_0)\beta_2(t)]\rho , \\ \beta_Y(t)\rho &= \frac{1}{2}\left[\frac{\gamma_a}{\hbar\omega_a}\right]^{1/2}\{\cos(\phi_0)[E_1(t),\rho]_+ \\ &\quad +\sin(\phi_0)[E_2(t),\rho]_+\} \\ &\equiv[\cos(\phi_0)\beta_1(t)+\sin(\phi_0)\beta_2(t)]\rho .\end{aligned} \tag{2.7}$$

The point in making these definitions is that we now have a commuting form of quantum noise, that is, the operators $\beta_X(t)$ and $\beta_Y(t)$ satisfy

$$\begin{aligned}[\beta_X(t),\beta_X(t')] &= [\beta_Y(t),\beta_Y(t')] \\ &= [\beta_X(t),\beta_Y(t')]=0\end{aligned} \tag{2.8}$$

for all t,t'. This implies that the equations can be treated as classical c-number equations, amenable to solution by ordinary stochastic methods. Hence, we need only specify the statistics of $\beta_X(t)$ and $\beta_Y(t)$, as determined by the initial quantum state of the incoming electric field (the bath).

B. Statistics of the squeezed-light source

The degenerate parametric amplifier will serve as our source of squeezed light. In practice this has proved to be the most successful source of squeezed light,[8] yielding results in reasonable agreement with theoretical predictions.[12] With the assumption that the amplifier is operating below threshold in a single-ended cavity (around the frequency ω_0), theoretical analyses yield for the correlation functions of the output light

$$\langle \beta_1(t)\beta_1(t')\rangle = \gamma_a \left[-\frac{\epsilon_c \gamma_c}{\gamma_c/2+\epsilon_c} e^{-(\gamma_c/2+\epsilon_c)|t-t'|} + \delta(t-t') \right]$$
$$= \gamma_a \left[-\frac{\lambda^2-\mu^2}{2\lambda} e^{-\lambda|t-t'|} + \delta(t-t') \right] ,$$
$$\langle \beta_1(t)\beta_1(t')\rangle = \gamma_a \left[-\frac{\epsilon_c \gamma_c}{\gamma_c/2+\epsilon_c} e^{-(\gamma_c/2+\epsilon_c)|t-t'|} + \delta(t-t') \right]$$
$$= \gamma_a \left[\frac{\lambda^2-\mu^2}{2\mu} e^{-\mu|t-t'|} + \delta(t-t') \right] ,$$
$$\langle \beta_1(t)\beta_2(t')\rangle = 0 , \tag{2.9}$$

where γ_c is the cavity damping, ϵ_c is the amplifier driving strength ($\epsilon_c > 0$), and

$$\lambda = \tfrac{1}{2}\gamma_c + \epsilon_c , \quad \mu = \tfrac{1}{2}\gamma_c - \epsilon_c .$$

The exponential terms in the expressions give the effect of squeezing, while the δ-correlated terms represent vacuum fluctuations. Strong squeezing is achieved in one quadrature as we approach threshold, i.e., as $\epsilon_c \to \frac{1}{2}\gamma_c$. In this limit, fluctuations in the unsqueezed quadrature become very large, and the correlation time of these fluctuations μ^{-1} approaches infinity. This effect has been shown to eventually cause a cessation of line narrowing in spontaneous emission and atomic absorption spectra in a squeezed vacuum of the form specified by the correlation functions (2.9).[9,10] However, we shall not be interested in this particular aspect of the squeezed-vacuum-atom interaction.

The white-noise limit, in which most previous work has been carried out, corresponds to the situation in which both λ and μ are much larger than any decay rates or rates of oscillation occurring in the atomic dynamics. In this case, we approximate the exponentials by δ-functions, giving

$$\langle \beta_1(t)\beta_1(t')\rangle = \gamma_a(2N-2M+1)\delta(t-t') ,$$
$$\langle \beta_2(t)\beta_2(t')\rangle = \gamma_a(2N+2M+1)\delta(t-t') , \tag{2.10}$$

where we have introduced the "standard" parameters N and M, defined by

$$N-M = -\frac{\lambda^2-\mu^2}{2\lambda^2} , \quad N+M = \frac{\lambda^2-\mu^2}{2\mu^2} , \tag{2.11}$$

with $M=[N(N+1)]^{1/2}$ (i.e., we assume a minimum uncertainty state).

Returning to the non-white-noise description, but retaining the N,M notation, we can now define the correlation properties of $\beta_X(t)$ and $\beta_Y(t)$. These take the form

$$\langle \beta_X(t)\beta_X(t')\rangle = \gamma_a \sin^2(\phi_0)(N-M)\lambda e^{-\lambda|t-t'|} + \gamma_a \cos^2(\phi_0)(N+M)\mu e^{-\mu|t-t'|} + \gamma_a \delta(t-t') ,$$
$$\langle \beta_Y(t)\beta_Y(t')\rangle = \gamma_a \cos^2(\phi_0)(N-M)\lambda e^{-\lambda|t-t'|} + \gamma_a \sin^2(\phi_0)(N+M)\mu e^{-\mu|t-t'|} + \gamma_a \delta(t-t') , \tag{2.12}$$
$$\langle \beta_X(t)\beta_Y(t')\rangle = -\frac{\gamma_a}{2}\sin(2\phi_0)(N-M)\lambda e^{-\lambda|t-t'|} + \frac{\gamma_a}{2}\sin(2\phi_0)(N+M)\mu e^{-\mu|t-t'|} .$$

Finally, we note that in specifying the correlations (2.9) and (2.12), we have made a particular choice of phase for the squeezed vacuum. This does not lead to a loss of generality, as the dynamics are sensitive only to the relative phase between the coherent driving field and the squeezed vacuum. This relative phase can be controlled through the phase of the coherent field ϕ_0. In an experimental situation, we would envisage a single laser providing the pump for both the atoms and the parametric amplifier.

III. SOLUTIONS TO THE EQUATIONS OF MOTION

Before commencing our analysis of the equations of motion, we find it convenient to average firstly over the white-noise portions of $\beta_X(t)$ and $\beta_Y(t)$. We do this by writing $\beta_X(t)$ as a sum of independent colored and white-noise sources:

$$\beta_X(t) = \beta_X^c(t) + \beta_X^\omega(t) , \tag{3.1}$$

with

$$\langle \beta_X^\omega(t)\beta_X^\omega(t')\rangle = \gamma_a \delta(t-t') ,$$
$$\langle \beta_X^c(t)\beta_X^c(t')\rangle = \gamma_a \sin^2(\phi_0)(N-M)\lambda e^{-\lambda|t-t'|} + \gamma_a \cos^2(\phi_0)(N+M)\mu e^{-\mu|t-t'|} , \tag{3.2}$$

and similarly for $\beta_Y(t)$. The Equations (2.6) are in the form of Stratonovich stochastic differential equations. For the purpose of averaging over the white noises $\beta_X^\omega(t)$ and $\beta_Y^\omega(t)$, we convert to the Ito form of the stochastic equations[13] (with respect to the white noises). Averaging is then straightforward and results in the equations

$$\dot{\bar{S}}_x = -\frac{\gamma_a}{2}\bar{S}_x - \Delta_a \bar{S}_y - \beta_X^c(t)\bar{S}_z ,$$
$$\dot{\bar{S}}_y = -\frac{\gamma_a}{2}\bar{S}_y + \Delta_a \bar{S}_x - \Omega_0 \bar{S}_z - \beta_Y^c(t)\bar{S}_z , \tag{3.3}$$
$$\dot{\bar{S}}_z = -\gamma_a - \gamma_a \bar{S}_z + \Omega_0 \bar{S}_y + \beta_X^c(t)\bar{S}_x + \beta_Y^c(t)\bar{S}_y ,$$

where the bar is now understood to incorporate the white-noise average. It remains therefore to perform the average over $\beta_X^c(t)$ and $\beta_Y^c(t)$ to obtain $\langle S_i(t)\rangle$, where $\langle\ \rangle$ denotes the total average.

Considerable insight into the nature of our problem can be gained from a simple qualitative inspection of the

equations (3.3). In the lowest order (neglecting noise terms), and for zero detuning, $\langle S_x(t)\rangle$ displays a simple exponential decay, while $\langle S_y(t)\rangle$ and $\langle S_z(t)\rangle$ undergo Rabi oscillations at frequency Ω_0 (in the rotating frame) and also decay exponentially. The contribution to the time development of $\langle S_x(t)\rangle$ from the additional noise terms is proportional to the time average of $\beta_X^c(t)\bar{S}_z(t)$. Since $\bar{S}_z(t)$ undergoes Rabi oscillations, it follows that this contribution will be significant only if $\beta_X^c(t)$ contains Fourier components at the frequencies $\pm\Omega_0$. Clearly, if $\beta_X^c(t)$ is a narrow-bandwidth noise source, with significant spectral components only at frequencies much smaller than Ω_0, then this term will play little part in the time evolution of $\langle S_x(t)\rangle$. A similar argument can be applied to $\langle S_y(t)\rangle$ and $\langle S_z(t)\rangle$. The time development of both $\langle S_y(t)\rangle$ and $\langle S_z(t)\rangle$ will be sensitive to the spectral components of $\beta_Y^c(t)$ around zero frequency, while in the equation of motion for $\bar{S}_z(t)$, the term $\beta_X^c(t)\bar{S}_x(t)$ will be significant only if, once again, $\beta_X^c(t)$ has non-negligible frequency components at $\pm\Omega_0$. Hence, $\langle S_y(t)\rangle$ and $\langle S_z(t)\rangle$ will be sensitive to spectral components of the noise sources at both zero frequency and at the frequencies $\pm\Omega_0$.

The above argument raises the interesting possibility of effectively decoupling the noise source $\beta_X^c(t)$ from the dynamics of the atom. This possibility takes on special significance in the case of a squeezed vacuum input when, through an appropriate choice of phase ϕ_0, the unsqueezed (noisy) quadrature can be made to correspond to $\beta_X^c(t)$. We shall now investigate this possibility, firstly by using an approximate analytical method, and then by direct numerical simulation of the equations (3.3).

A. Decorrelation approximation

The basic features of our problem can be illustrated using a straightforward decorrelation-approximation approach, whereby the noise sources and system variables are assumed to decorrelate under averaging. Briefly, we solve for two of the system variables and substitute the results into the equation of motion for the third variable, after which averaging is performed in the decorrelation approximation. Two distinct limiting cases characterize our problem, corresponding to the choices of phase $\phi_0=0$ and $\phi_0=\pi/2$. For simplicity, we shall consider only these two cases, and therefore we have

$$\begin{aligned}
&\langle \beta_X^c(t)\beta_X^c(t')\rangle = \gamma_a(N\pm M)b_\pm e^{-b_\pm|t-t'|}\,,\\
&\langle \beta_Y^c(t)\beta_Y^c(t')\rangle = \gamma_a(N\mp M)b_\mp e^{-b_\mp|t-t'|}\,,\\
&\langle \beta_X^c(t)\beta_Y^c(t')\rangle = 0\,,
\end{aligned} \tag{3.4}$$

where $b_+=\mu$ and $b_-=\lambda$. With the further assumption of a strong driving field ($\Omega_0 \gg \gamma_a/4$), we find, after some work,

$$\begin{aligned}
\langle \dot{S}_x(t)\rangle = &-\frac{\gamma_a}{2}\langle S_x(t)\rangle + \gamma_a(N\pm M)b_\pm \int_0^t dt'\, e^{-(3\gamma_a/4+b_\pm)(t-t')}\frac{\gamma_a}{4\Omega_0}\sin[\Omega_0(t-t')]\langle S_x(t')\rangle\\
&-\gamma_a(N\pm M)b_\pm \int_0^t dt'\, e^{-(3\gamma_a/4+b_\pm)(t-t')}\cos[\Omega_0(t-t')]\langle S_x(t')\rangle\,,
\end{aligned} \tag{3.5a}$$

$$\begin{aligned}
\langle \dot{S}_y(t)\rangle = &-\frac{\gamma_a}{2}\langle S_y(t)\rangle + \gamma_a(N\mp M)b_\mp \int_0^t dt'\, e^{-(3\gamma_a/4+b_\mp)(t-t')}\frac{\gamma_a}{4\Omega_0}\sin[\Omega_0(t-t')]\langle S_y(t')\rangle\\
&-\gamma_a(N\mp M)b_\mp \int_0^t dt'\, e^{-(3\gamma_a/4+b_\mp)(t-t')}\cos[\Omega_0(t-t')]\langle S_y(t')\rangle\\
&-\Omega_0\langle S_z(t)\rangle + \gamma_a(N\mp M)b_\mp \int_0^t dt'\, e^{-(3\gamma_a/4+b_\mp)(t-t')}\sin[\Omega_0(t-t')]\langle S_z(t')\rangle\,,
\end{aligned} \tag{3.5b}$$

$$\begin{aligned}
\langle \dot{S}_z(t)\rangle = &-\gamma_a - \gamma_a\langle S_z(t)\rangle - \gamma_a(N\pm M)b_\pm \int_0^t dt'\, e^{-(\gamma_a/2+b_\pm)(t-t')}\langle S_z(t')\rangle\\
&-\gamma_a(N\mp M)b_\mp \int_0^t dt'\, e^{-(3\gamma_a/4+b_\mp)(t-t')}\frac{\gamma_a}{4\Omega_0}\sin[\Omega_0(t-t')]\langle S_z(t')\rangle\\
&-\gamma_a(N\mp M)b_\mp \int_0^t dt'\, e^{-(3\gamma_a/4+b_\mp)(t-t')}\cos[\Omega_0(t-t')]\langle S_z(t')\rangle\\
&+\Omega_0\langle S_y(t)\rangle - \gamma_a(N\mp M)b_\mp \int_0^t dt'\, e^{-(3\gamma_a/4+b_\mp)(t-t')}\sin[\Omega_0(t-t')]\langle S_y(t')\rangle\,.
\end{aligned} \tag{3.5c}$$

In the white-noise limit, one has $b_\pm \gg \Omega_0$, and to a good approximation $\langle S_i(t')\rangle$ can be replaced in the integrals by $\langle S_i(t)\rangle$. However, we are interested in the opposite limit, $\Omega_0 \gg b_\pm$. Provided b_+ and b_- are larger than the decay rates of the various spin components, then the appropriate substitutions in this limit are

$$\begin{aligned}
&\langle S_x(t')\rangle \approx \langle S_x(t)\rangle\,,\\
&\langle S_y(t')\rangle \approx \cos[\Omega_0(t-t')]\langle S_y(t)\rangle + \sin[\Omega_0(t-t')]\langle S_z(t)\rangle\,,\\
&\langle S_z(t')\rangle \approx \cos[\Omega_0(t-t')]\langle S_z(t)\rangle - \sin[\Omega_0(t-t')]\langle S_y(t)\rangle\,.
\end{aligned} \tag{3.6}$$

The integrals that remain can then be evaluated. The time-dependent terms that result from the integrals are assumed to give only small transient effects, and so we neglect them. Hence, we establish the modified Bloch equations

$$\begin{aligned}
\langle \dot{S}_x \rangle &\simeq -\gamma_x \langle S_x \rangle \ , \\
\langle \dot{S}_y \rangle &\simeq -\gamma_y \langle S_y \rangle - \Omega_z \langle S_z \rangle \ , \\
\langle \dot{S}_z \rangle &\simeq -\gamma_a - \gamma_z \langle S_z \rangle + \Omega_y \langle S_y \rangle \ ,
\end{aligned} \tag{3.7}$$

where

$$\begin{aligned}
\gamma_x &= \frac{\gamma_a}{2}\left[1+2(N\pm M)\frac{b_\pm(b_\pm+\gamma_a/2)}{(b_\pm+3\gamma_a/4)^2+\Omega_0^2}\right] , \\
\gamma_y &= \frac{\gamma_a}{2}\left[1+2(N\mp M)\frac{b_\mp}{b_\mp+3\gamma_a/4}\right. \\
&\qquad \left. -(N\mp M)\frac{\gamma_a b_\mp/2}{(b_\mp+3\gamma_a/4)^2+4\Omega_0^2}\right] , \\
\gamma_z &= \gamma_a\left[1+(N\mp M)\frac{b_\mp}{b_\mp+3\gamma_a/4}\right. \\
&\qquad +(N\mp M)\frac{b_\mp\gamma_a/4}{(b_\mp+3\gamma_a/4)^2+4\Omega_0^2} \\
&\qquad \left. +(N\pm M)\frac{b_\pm(b_\pm+\gamma_a/2)}{(b_\pm+\gamma_a/2)^2+\Omega_0^2}\right] ,
\end{aligned} \tag{3.8}$$

and

$$\begin{aligned}
\Omega_z &= \Omega_0\left[1-(N\mp M)\frac{\gamma_a^2}{8\Omega_0^2}\frac{b_\mp}{b_\mp+3\gamma_a/4}\right. \\
&\qquad \left. +(N\mp M)\frac{\gamma_a^2}{8\Omega_0^2}\frac{b_\mp(b_\mp+3\gamma_a/4)}{(b_\mp+3\gamma_a/4)^2+4\Omega_0^2}\right] , \\
\Omega_y &= \Omega_0\left[1+(N\mp M)\frac{\gamma_a^2}{8\Omega_0^2}\frac{b_\mp}{b_\mp+3\gamma_a/4}\right. \\
&\qquad -(N\mp M)\frac{\gamma_a^2}{8\Omega_0^2}\frac{b_\mp(b_\mp+3\gamma_a/4)}{(b_\mp+3\gamma_a/4)^2+4\Omega_0^2} \\
&\qquad \left. +(N\pm M)\frac{\gamma_a b_\pm}{(b_\pm+\gamma_a/2)^2+\Omega_0^2}\right] .
\end{aligned} \tag{3.9}$$

In view of the limit we are considering ($\Omega_0 \gg b_\pm$), many of the terms appearing in (3.8) and (3.9) are negligible. Removing these terms, we arrive finally at the results

$$\begin{aligned}
\gamma_x &\approx \frac{\gamma_a}{2} \ , \\
\gamma_y &\approx \frac{\gamma_a}{2}\left[1+2(N\mp M)\frac{b_\mp}{b_\mp+3\gamma_a/4}\right] , \\
\gamma_z &\approx \gamma_a\left[1+(N\mp M)\frac{b_\mp}{b_\mp+3\gamma_a/4}\right] ,
\end{aligned} \tag{3.10}$$

and

$$\Omega_z \approx \Omega_y \approx \Omega_0 \ . \tag{3.11}$$

These permit the following observations:

(i) The component $\langle S_x(t) \rangle$ is damped at its normal vacuum rate independent of the choice of phase. This is to be expected, as the spectral distribution of the noises $\beta_X^c(t)$ and $\beta_Y^c(t)$ does not extend to the frequencies $\pm\Omega_0$. In the fluorescence spectrum, we can therefore expect the central peak of the Mollow triplet to remain unchanged.

(ii) The components $\langle S_y(t) \rangle$ and $\langle S_z(t) \rangle$ are damped at the rate

$$\tfrac{1}{2}(\gamma_y+\gamma_z) = \frac{3\gamma_a}{4} + \gamma_a(N\mp M)\frac{b_\mp}{b_\mp+3\gamma_a/4} \ , \tag{3.12}$$

which, if we consider the optimum case, $b_\mp \gg \gamma_a$, can be further simplified to

$$\tfrac{1}{2}(\gamma_y+\gamma_z) \approx \gamma_a(\tfrac{3}{4}+N\mp M) \ . \tag{3.13}$$

For large squeezing ($N \gg 1$), we have

$$\begin{aligned}
N-M &\approx -\tfrac{1}{2}+\frac{1}{8N} \ , \\
N+M &\approx 2N+\tfrac{1}{2} \ ,
\end{aligned} \tag{3.14}$$

and hence the two choices of phase lead to widely different behavior. For the case $\phi_0=0$,

$$\tfrac{1}{2}(\gamma_y+\gamma_z) \approx \gamma_a\left[\frac{1}{4}+\frac{1}{8N}\right] , \tag{3.15}$$

and the decay of $\langle S_y(t) \rangle$ and $\langle S_z(t) \rangle$ is found to be *inhibited* from its normal vacuum rate by an amount which could approach 66%. It follows that the Rabi sidebands should be *narrowed* compared to their natural width. For the case $\phi_0=\pi/2$,

$$\tfrac{1}{2}(\gamma_y+\gamma_z) \approx 2N\gamma_a \ , \tag{3.16}$$

and the decay rate is greatly enhanced, leading to a broadening of the Rabi peaks.

(iii) These results are in marked contrast to those found in the white-noise limit, where $b_\pm \gg \Omega_0$.[2] In particular, one finds, for $\phi_0=0$ (and for $N \gg 1$),

$$\begin{aligned}
\gamma_x &= \gamma_a\left[N+M+\tfrac{1}{2}\right] \approx 2N\gamma_a \ , \\
\tfrac{1}{2}(\gamma_y+\gamma_z) &= \gamma_a\left[\tfrac{3}{2}N-\tfrac{1}{2}M+\tfrac{3}{4}\right] \approx N\gamma_a \ ,
\end{aligned} \tag{3.17}$$

while for $\phi_0=\pi/2$,

$$\begin{aligned}
\gamma_x &= \gamma_a\left[N-M+\tfrac{1}{2}\right] \approx \frac{\gamma_a}{8N} \ , \\
\tfrac{1}{2}(\gamma_y+\gamma_z) &= \gamma_a\left[\tfrac{3}{2}N+\tfrac{1}{2}M+\tfrac{3}{4}\right] \approx 2N\gamma_a \ .
\end{aligned} \tag{3.18}$$

Hence, for strong squeezing, the central peak can be narrowed with an appropriate choice of phase ($\phi_0=\pi/2$), but the sidebands can only be broadened relative to their natural width.

B. Solution via stochastic simulation

In a previous study of the effect of finite-bandwidth squeezing on atomic phase decays,[9] the technique of stochastic simulation was successfully employed to establish solutions to the equations of motion, and to compute two-time correlation functions (and hence spectra). We shall now adopt this technique once more to provide confirmation of the approximate analytical results found in the previous section.

The equations (3.3) are simulated using a fully implicit numerical integration scheme.[14] This scheme approximates the equations with the form

$$\begin{aligned}\Delta\mathbf{S}^n&=\mathbf{S}^{n+1}-\mathbf{S}^n\\&=\mathbf{A}(\mathbf{S}^{n+\theta_1})\Delta t+\mathbf{B}(\mathbf{S}^{n+\theta_2})\beta_X^{c,n}\Delta t\\&\quad+\mathbf{C}(\mathbf{S}^{n+\theta_2})\beta_Y^{c,n}\Delta t\ ,\end{aligned}\tag{3.19}$$

where

$$\mathbf{S}=\begin{bmatrix}\bar{S}_x\\ \bar{S}_y\\ \bar{S}_z\end{bmatrix}\ ,\tag{3.20}$$

$$\mathbf{A}(\mathbf{S})=\begin{bmatrix}-\frac{\gamma_a}{2}\bar{S}_x-\Delta_a\bar{S}_y\\ -\frac{\gamma_a}{2}\bar{S}_y+\Delta_a\bar{S}_x-\Omega_0\bar{S}_z\\ -\gamma_a-\gamma_a\bar{S}_z+\Omega_0\bar{S}_y\end{bmatrix}\ ,$$

$$\mathbf{B}(\mathbf{S})=\begin{bmatrix}-\bar{S}_z\\ 0\\ \bar{S}_x\end{bmatrix}\ ,\tag{3.21}$$

$$\mathbf{C}(\mathbf{S})=\begin{bmatrix}0\\ -\bar{S}_z\\ \bar{S}_y\end{bmatrix}\ ,$$

Δt is the time step, $\theta_1,\ \theta_2\in[0,1]$, and

$$\mathbf{A}(\mathbf{S}^{n+\theta_1})=\mathbf{A}(\mathbf{S}^n)+\underline{J}_A^n\theta_1\Delta\mathbf{S}^n\ ,\quad(\underline{J}_A^n)_{ij}=\left[\frac{\partial A_i}{\partial S_j}\right]_{\mathbf{S}=\mathbf{S}^n}\ ,\tag{3.22}$$

$$\mathbf{B}(\mathbf{S}^{n+\theta_2})=\mathbf{B}(\mathbf{S}^n)+\underline{J}_B^n\theta_2\Delta\mathbf{S}^n\ ,\quad(\underline{J}_B^n)_{ij}=\left[\frac{\partial B_i}{\partial S_j}\right]_{\mathbf{S}=\mathbf{S}^n}\ ,\tag{3.23}$$

$$\mathbf{C}(\mathbf{S}^{n+\theta_2})=\mathbf{C}(\mathbf{S}^n)+\underline{J}_C^n\theta_2\Delta\mathbf{S}^n\ ,\quad(\underline{J}_C^n)_{ij}=\left[\frac{\partial C_i}{\partial S_j}\right]_{\mathbf{S}=\mathbf{S}^n}\ ,$$

(i.e., we linearize about the point $\mathbf{S}^n$). It is straightforward to show that

$$\underline{J}_A^n=\begin{bmatrix}-\gamma_a/2 & -\Delta_a & 0\\ \Delta_a & -\gamma_a/2 & -\Omega_0\\ 0 & \Omega_0 & -\gamma_a\end{bmatrix}\ ,$$

$$\underline{J}_B^n=\begin{bmatrix}0&0&-1\\0&0&0\\1&0&0\end{bmatrix}\ ,\tag{3.24}$$

$$\underline{J}_C^n=\begin{bmatrix}0&0&0\\0&0&-1\\0&1&0\end{bmatrix}\ .$$

Substitution of (3.22) and (3.23) into (3.19) leads to the integration scheme

$$\begin{aligned}\Delta\mathbf{S}^n=&[1-\theta_1\underline{J}_A^n\Delta t-\theta_2\underline{J}_B^n\beta_X^{c,n}\Delta t-\theta_2\underline{J}_C^n\beta_Y^{c,n}\Delta t]^{-1}\\&\times[\mathbf{A}(\mathbf{S}^n)\Delta t+\mathbf{B}(\mathbf{S}^n)\beta_X^{c,n}\Delta t+\mathbf{C}(\mathbf{S}^n)\beta_Y^{c,n}\Delta t]\ .\end{aligned}\tag{3.25}$$

The choice $\theta_1=\theta_2=0$ corresponds to the Euler method of integration. This method, however, can suffer stability problems, especially when large Rabi frequencies are involved, and hence we have opted in general for the time-centered choice $\theta_1=\theta_2=\frac{1}{2}$. This fully implicit method has very good stability properties, and is appropriate for the integration of the Stratonovich stochastic differential equations we are dealing with here.

Noise sources with the correct statistics are constructed using summations of suitably weighted Gaussian distributed random numbers. The negative correlations which characterize squeezing require that these sources be complex. This enables $\bar{S}_x(t)$, $\bar{S}_y(t)$, and $\bar{S}_z(t)$ to develop imaginary parts, but in practice these average to zero after a sufficient number of trials, provided that the integration routine is stable.

1. *Results for* $\langle S_z(t)\rangle$

The averages $\langle S_i(t)\rangle$ $(i=x,y,z)$ have typically been computed from 5000 trajectories. Our first aim is to confirm the basic predictions of Sec. III A, and so, for Fig. 1, we have chosen parameters to roughly suit the assumptions made in obtaining the approximate analytical results (i.e., $\Omega_0\gg b_+,\ b_-\gg\gamma_a$). The decay of $\langle S_z(t)\rangle$ is clearly inhibited or enhanced, depending on the choice of phase. An approximate fit to the curves yields decay rates of $0.32\gamma_a$ and $4.9\gamma_a$ for $\phi_0=0$ and $\phi_0=\pi/2$, respectively. These can be compared with the approximate theoretical result (3.12), which predicts decay rates of $0.35\gamma_a$ $(N-M=-0.44)$ and $3.8\gamma_a$ $(N+M=4)$.

In Fig. 2, we demonstrate that inhibition and enhancement of the decay rate persists even when the bandwidth of squeezed light is only marginally greater than γ_a. We consider the case $\Omega_0=20\gamma_a$, with $\gamma_c=3\gamma_a$, $\epsilon_c=0.75\gamma_a$ $(b_+=0.75\gamma_a,\ b_-=2.25\gamma_a)$, and find inhibited and enhanced decay rates of $0.32\gamma_a$ and $3.2\gamma_a$, respectively. The result (3.12) predicts, for these parameters, the rates $0.42\gamma_a$ and $2.8\gamma_a$, but it is likely that we are approaching the limits of validity of this theory. Indeed, as we in-

crease the parametric driving strength ϵ_c further, an optimum value is reached, $\epsilon_c \approx \gamma_a$ (at which inhibition is maximized), after which the degree of inhibition is reduced.

2. *Correlation functions and spectra*

The computation of correlation functions and spectra is somewhat more difficult than the evaluation of the simple spin averages. In particular, the non-Markov nature of the processes being studied means that the familiar quantum regression theorem cannot be applied. In Ref. 9, methods are developed for the simulation of the correlation functions, from which spectra are computed using a fast Fourier-transform routine. There it is shown that if the solutions of the equations of motion (3.3) are written in the form

$$\bar{S}_i(t) = \sum_j f_{ij}(t,t')\bar{S}_j(t') + g_i(t,t') , \tag{3.26}$$

then the stationary correlation functions are given by

$$\langle S_i(t)S_k(t')\rangle = \langle f_{ik}(t,t')\rangle + \langle g_i(t,t')g_k^{\rm st}(t')\rangle + i\sum_{l,m} \epsilon_{lkm}\langle f_{il}(t,t')g_m^{\rm st}(t')\rangle , \tag{3.27}$$

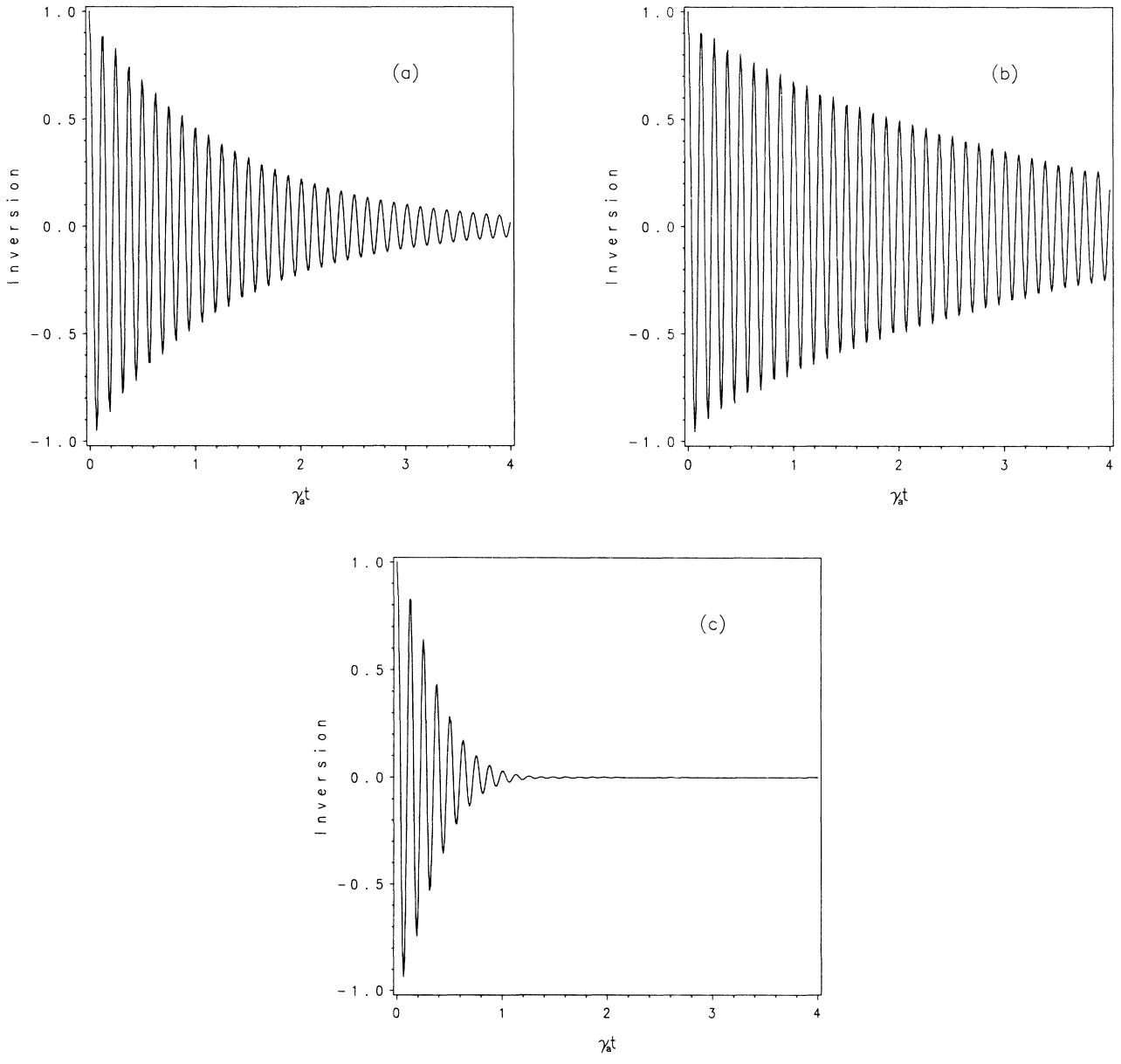

FIG. 1. Population inversion $\langle S_z(t)\rangle$ computed by simulation for $\Omega_0 = 50\gamma_a$, $\gamma_c = 10\gamma_a$, with (a) $\epsilon_c = 0$ (no squeezing), (b) $\epsilon_c = 2.5\gamma_a$ (89% squeezing), $\phi_0 = 0$, (c) $\epsilon_c = 2.5\gamma_a$, $\phi_0 = \pi/2$. The squeezing bandwidths in the two quadratures are $b_+ = 2.5\gamma_a$, $b_- = 7.5\gamma_a$.

where $g_i(t,t') \rightarrow g_i^{st}(t)$ as $t \rightarrow \infty$.

To evaluate (3.27) from the stochastic simulation, we first allow the equations to evolve to a stationary state, thereby obtaining $g_i^{st}(t')$. A new trajectory is then initiated, with four different sets of initial conditions, so that we may identify $f_{ij}(t,t')$ and $g_i(t,t')$. The procedure is then repeated, and after approximately 10 000 trials, the average is taken. We remove the coherent contribution to the correlation functions, and sample to a time at which the correlation functions are small (so as to avoid aliasing in the fast Fourier transform).

In our first series of graphs, in Figs. 3–5, we return to the squeezing parameters of Fig. 1, and consider the variation in the fluorescence spectrum with changing Ω_0. For $\Omega_0=50\gamma_a$ [Figs. 3–5(c)] and $\Omega_0=20\gamma_a$ [Figs. 3–5(b)], the Rabi sideband narrowing and/or broadening we have described in previous sections is the dominant feature, with the central peak essentially unchanged from its normal vacuum form. However, for $\Omega_0=10\gamma_a$ [Figs. 3–5(a)], we start to see features which characterize the white-noise results, since now the bandwidth of squeezed light is comparable to the Rabi splitting. The Rabi side-

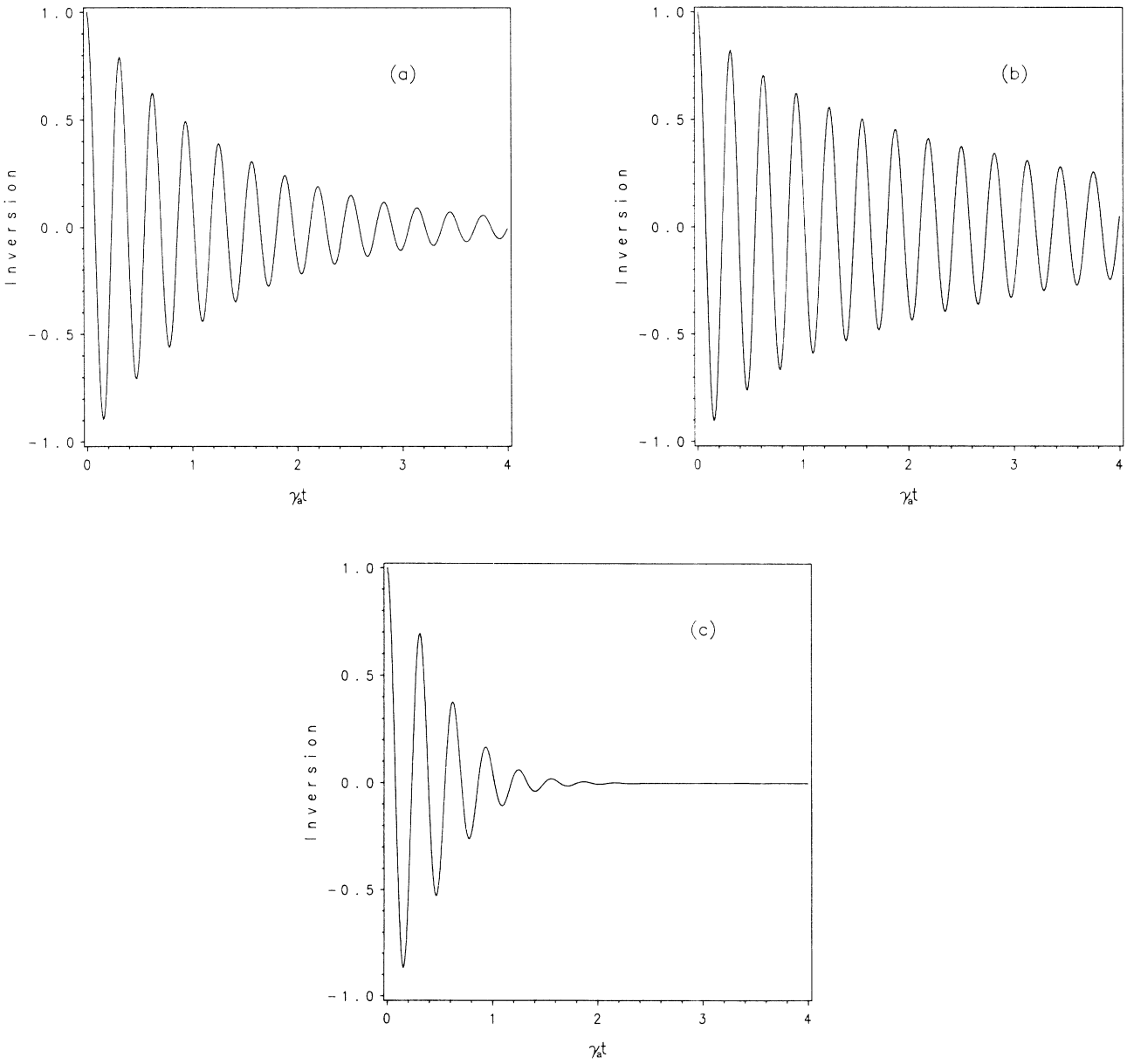

FIG. 2. Population inversion $\langle S_z(t) \rangle$ computed by simulation for $\Omega_0=20\gamma_a$, $\gamma_c=3\gamma_a$, with (a) $\epsilon_c=0$ (no squeezing), (b) $\epsilon_c=0.75\gamma_a$ (89% squeezing), $\phi_0=0$, (c) $\epsilon_c=0.75\gamma_a$, $\phi_0=\pi/2$. The squeezing bandwidths in the two quadratures are $b_+=0.75\gamma_a$, $b_-=2.25\gamma_a$.

bands are, for the choice of phase $\phi_0=0$, no longer significantly narrowed compared to their natural width, and the width of the central peak is now strongly phase dependent, alternating between supernatural and subnatural values for $\phi_0=0$ and $\phi_0=\pi/2$, respectively.

In Fig. 5, where we concentrate on the Rabi peaks of Fig. 3, comparing them in each case with the normal (unsqueezed) vacuum result, we also note a slight shift in the position of the sidebands with the addition of squeezing. The width of the peak for $\Omega_0=50\gamma_a$ agrees well with the decay rate computed earlier from the behavior of $\langle S_z(t)\rangle$.

Finally, in Fig. 6, we plot the spectra obtained with the narrower-bandwidth squeezed light considered in Fig. 2, and for two values of the Rabi frequency $\Omega_0=10\gamma_a$ and $\Omega_0=20\gamma_a$. Again, the sideband narrowing is enhanced as Ω_0 is increased.

3. *Reflections*

Reflections of the input in the output field can play an important role in the case of squeezed inputs,[9,15] since the squeezed vacuum possesses a nontrivial power spectrum. As well as incorporating this into the total output-field

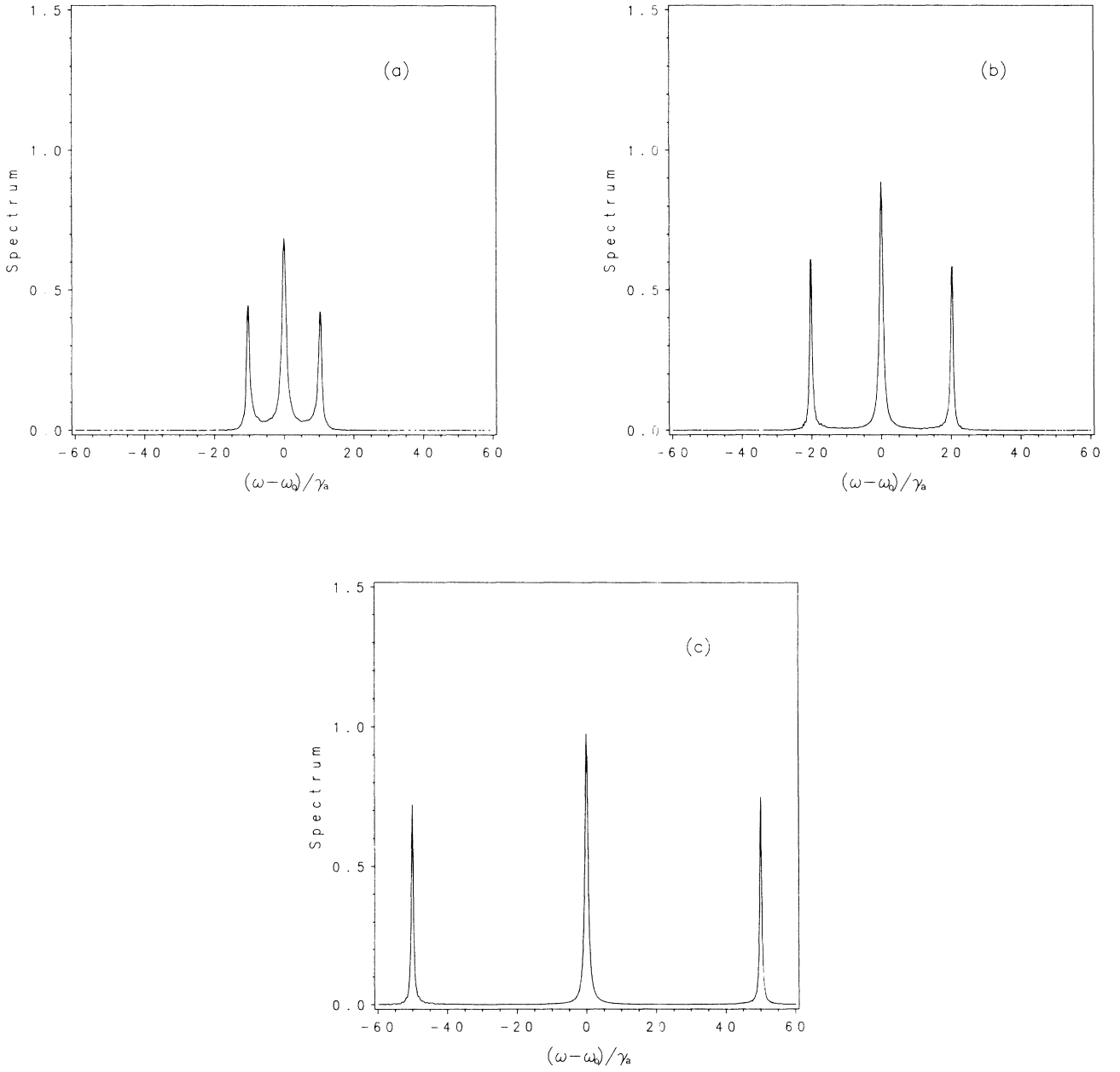

FIG. 3. Fluorescence spectrum, omitting reflections, computed by simulation for $\gamma_c=10\gamma_a$, $\epsilon_c=2.5\gamma_a$, $\phi_0=0$, with (a) $\Omega_0=10\gamma_a$, (b) $\Omega_0=20\gamma_a$, (c) $\Omega_0=50\gamma_a$.

spectrum, one must also allow for correlations between the reflected input field and the fluorescence from the atom. These correlations can lead to significant modifications of the total fluorescence spectrum.[9]

The reflections could, in principle, be avoided with the introduction of a small "window" of unsqueezed vacuum modes through which to observe the fluorescence[2] (small because we are assuming that the atom sees only squeezed vacuum modes). In any case, we have investigated (by simulation) the effect of reflections on the total fluorescence spectrum, and we find that, in our domain of interest ($\Omega_0 \gg b_\pm$), the Rabi peaks are unaffected, while the central peak is dominated by the squeezed vacuum spectrum, (i.e., by a Lorentzian of width $b_+ \equiv \mu$). Hence, the significant features of our work, Rabi sideband narrowing and broadening, can still be seen in the fluorescence spectrum when reflections of the input are included.

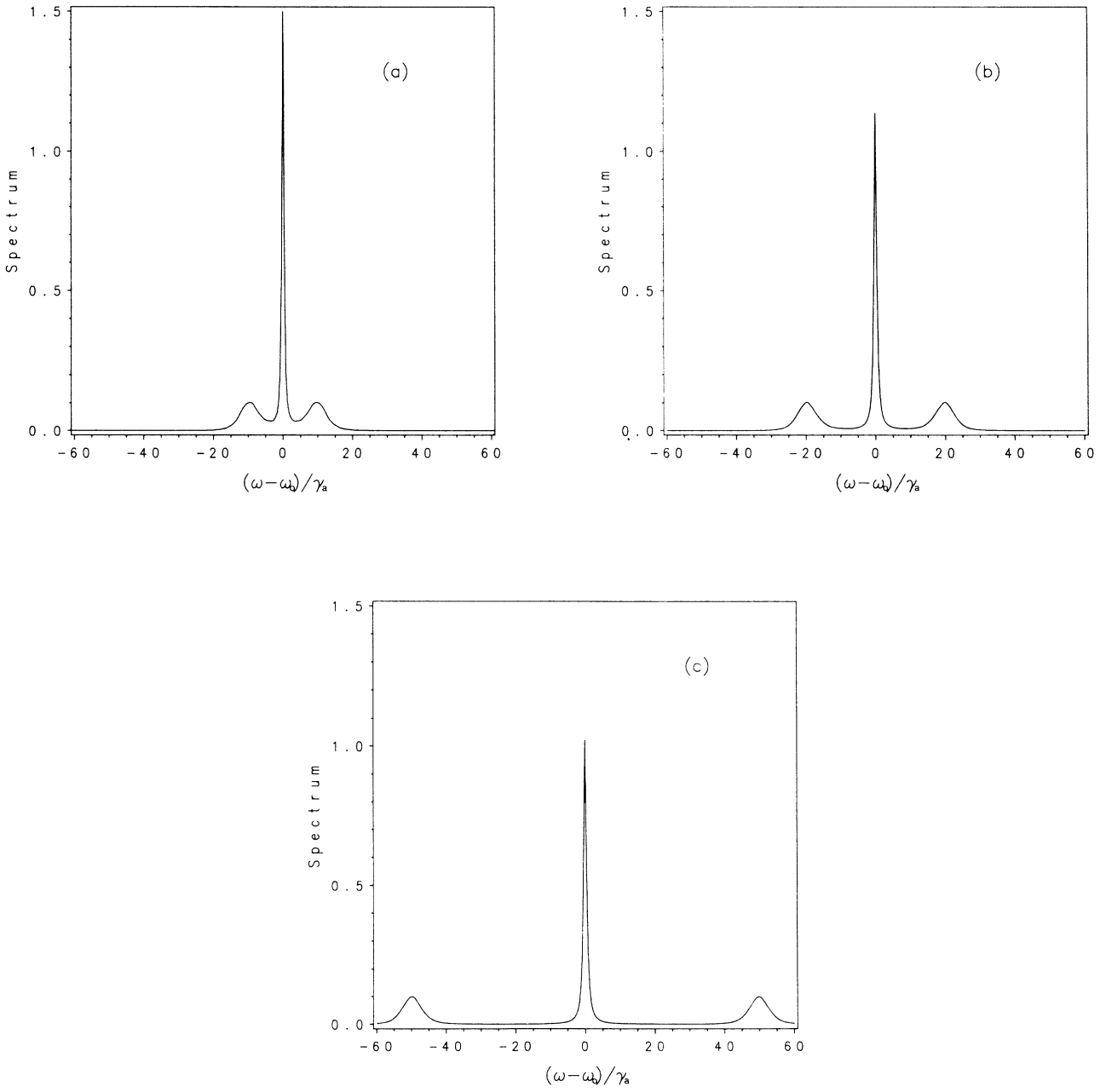

FIG. 4. Fluorescence spectrum, omitting reflections, computed by simulation for $\gamma_c = 10\gamma_a$, $\epsilon_c = 2.5\gamma_a$, $\phi_0 = \pi/2$, with (a) $\Omega_0 = 10\gamma_a$, (b) $\Omega_0 = 20\gamma_a$, (c) $\Omega_0 = 50\gamma_a$.

IV. SQUEEZED-CAVITY DYNAMICS

The frequency-dependent spectral density exhibited by an optical cavity offers interesting possibilities for the strongly driven resonance fluorescence of a single, cavity-confined, two-level atom. An analysis of the form given at the beginning of Sec. III shows that the decay of the S_x component of the Bloch vector is triggered by cavity vacuum fluctuations at the frequencies $\omega_0 \pm \Omega_0$ (we assume resonance between the atom, cavity, and driving field), while the decay of the S_y and S_z components is in response to fluctuations at the frequencies ω_0 and $\omega_0 \pm \Omega_0$. As pointed out by Lewenstein *et al.*[11] if the Rabi frequency Ω_0 is much larger than the cavity linewidth Γ, the cavity vacuum fluctuations that trigger the decay of the S_x component will be negligible, and S_x can be expected to remain virtually constant (as regards decay into the cavity modes). However, the decay of the S_y and S_z components can still be driven by cavity vacuum fluctuations at the frequency ω_0, where the cavity spectral density reaches its peak. In terms of the spectrum of resonance fluorescence, these effects produce a dramatic narrowing of the central peak in the Mollow triplet, together with a limited narrowing of the Rabi sidebands.

Our interest in this particular problem stems from the fact that if we inject a broadband squeezed vacuum into

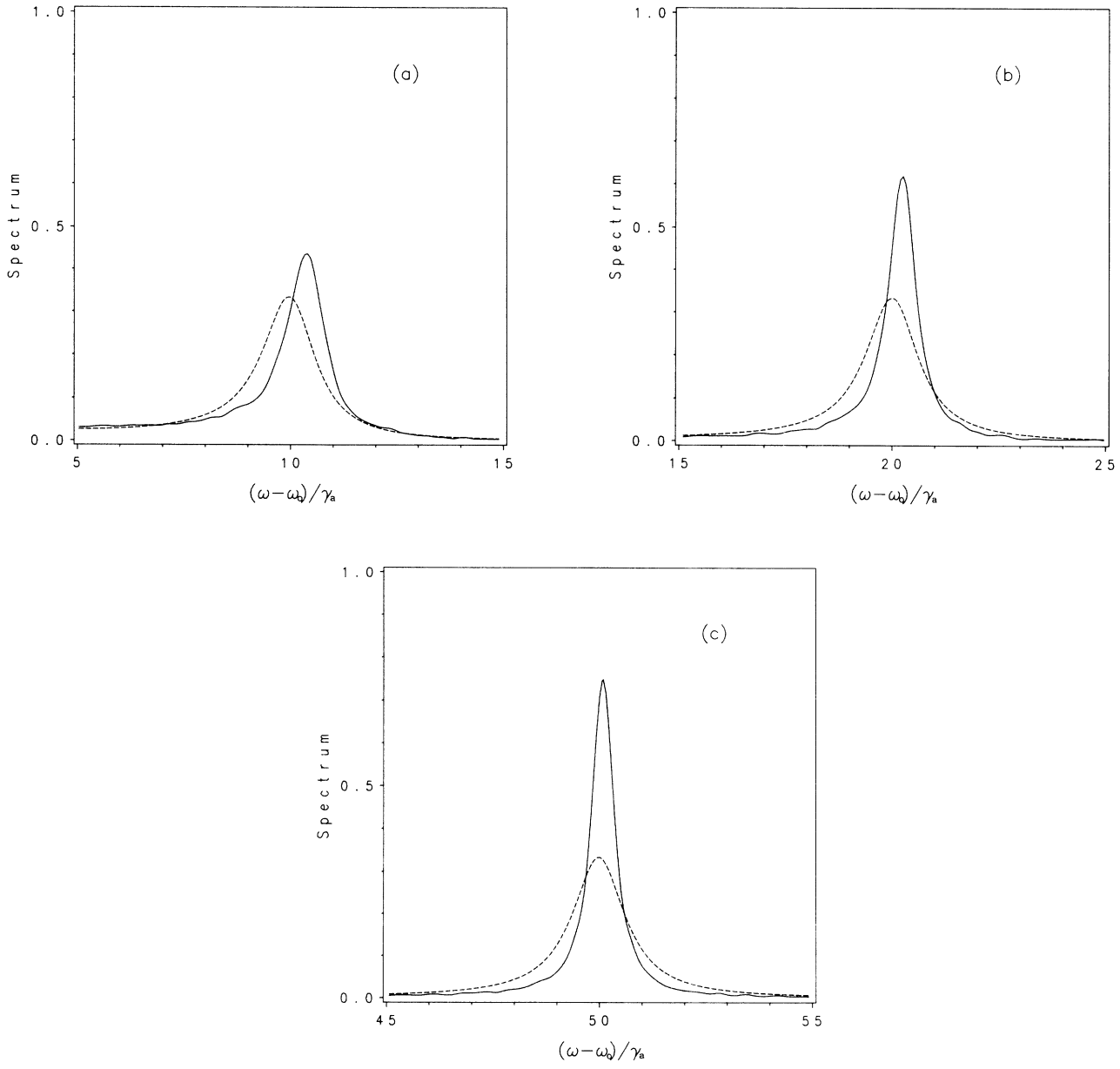

FIG. 5. Rabi sidebands of Fig. 3 compared with normal vacuum results (dashed lines).

the cavity, a cavity-confined atom can be made to experience squeezed vacuum fluctuations over a bandwidth Γ. If we consider the strong driving field limit $\Omega_0 \gg \Gamma$, then we have a close parallel with the work of Secs. II and III, except that now the vacuum fluctuations which could not be eliminated for that system (and gave a limit to how narrow we could make the peaks) are removed through the action of the cavity (i.e., the cavity does not support vacuum fluctuations at the frequencies $\omega_0 \pm \Omega_0$). Our previous results therefore lead us to postulate that the decay of all three components of the Bloch vector may be strongly inhibited through the combined action of the injected squeezed vacuum and the cavity spectral density.

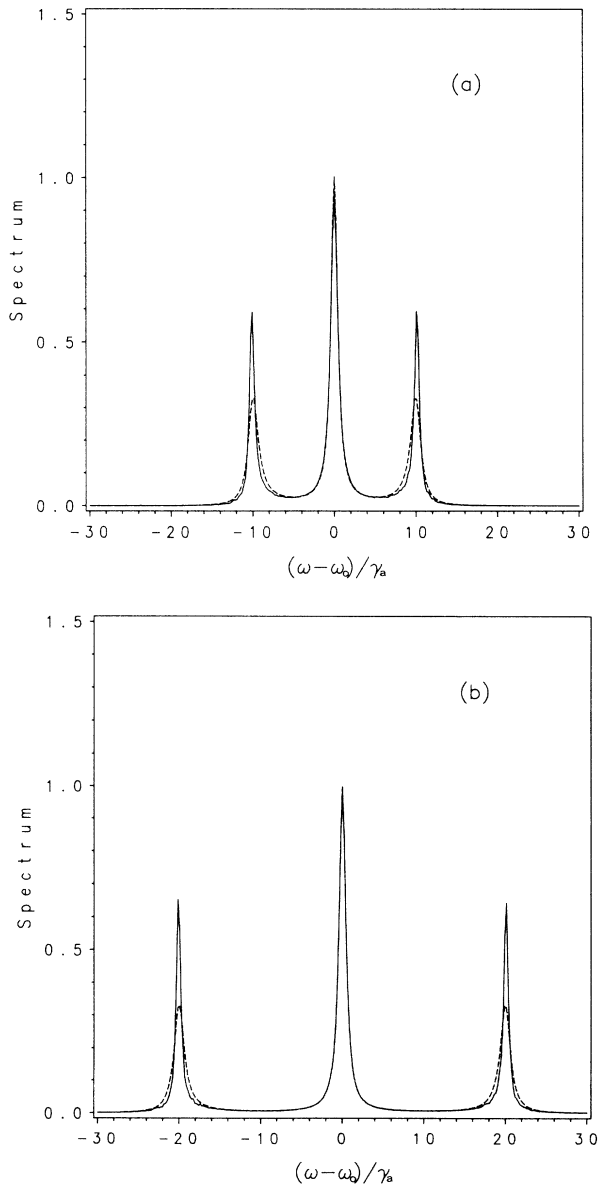

FIG. 6. Fluorescence spectrum, omitting reflections, computed by simulation for $\gamma_c = 3\gamma_a$, $\epsilon_c = 0.75\gamma_a$, $\phi_0 = 0$, with (a) $\Omega_0 = 10\gamma_a$, (b) $\Omega_0 = 20\gamma_a$, compared with normal vacuum results (dashed lines).

To confirm this prediction we shall closely follow the working of Lewenstein *et al.*[11]

A. Cavity model

We consider a single two-level atom located in the center of a cavity and driven by a laser field of frequency $\omega_0 = \omega_a$. The cavity spectral density is assumed to possess a peak centered on the frequency $\omega_c = \omega_0$. Adjacent peaks in the spectral density are ignored. We must also allow for coupling to those modes unassociated with the cavity (i.e., modes out the side of the cavity), and hence the reservoir is divided into two parts corresponding to the cavity (c_k) and background (b_k) modes, respectively. The Hamiltonian for this system is written (setting $\hbar = c = 1$), in the rotating wave approximation,

$$\begin{aligned} H = & \frac{\omega_a}{2} S_z + \int dk\, k c_k^\dagger c_k + \int dk\, k b_k^\dagger b_k \\ & + \frac{\Omega_0}{2}(S^- e^{i\omega_0 t - i\phi_0} + S^+ e^{-i\omega_0 t + i\phi_0}) \\ & + \int dk [g_c(k) S^+ c_k + \text{H.c.}] \\ & + \int dk [g_b(k) S^+ b_k + \text{H.c.}] \, . \end{aligned} \tag{4.1}$$

The coupling to each reservoir is described through the functions $g_c(k)$ and $g_b(k)$, which are proportional to the respective mode densities. The background modes correspond to a free-space reservoir and hence contribute equally at all frequencies in the vicinity of ω_0. Therefore, $g_b(k)$ can be regarded as constant, with

$$\int_{-\infty}^{\infty} dk\, |g_b(k)|^2 e^{-ik\tau} = \frac{\gamma_b}{2} \delta(\tau) \, , \tag{4.2}$$

where the frequency ω_0 corresponds to $k = 0$ in the rotating frame.

The function $|g_c(k)|^2$, representing the cavity-mode density, is modeled as a simple Lorentzian with a maximum value at the cavity resonance frequency. The Lorentzian has a half width at half maximum of Γ, and satisfies

$$\int_{-\infty}^{\infty} dk\, |g_c(k)|^2 e^{-ik\tau} = \frac{\gamma_c}{2} \Gamma e^{-\Gamma\tau} \, . \tag{4.3}$$

More precisely, we choose

$$g_c(k) = \left[\frac{\gamma_c}{2\pi} \right]^{1/2} \left[\frac{\Gamma}{\Gamma - ik} \right] \, . \tag{4.4}$$

The coefficients γ_b and γ_c give the contributions from the background and cavity modes to the overall (undriven) spontaneous emission rate of the atom. For significant effects to be observable, we will require γ_c to be at least comparable to γ_b. This should be achievable in practice with, for instance, confocal optical resonators.[16]

B. Modified Bloch equations

Following Lewenstein *et al.*, we derive standard Heisenberg equations of motion from the Hamiltonian (4.1), and eliminate the cavity and background photon operators through a first-order expansion in γ_c and γ_b (Born approximation). In doing so, we require that Γ and Ω_0 be much larger than γ_c and γ_b, but we do not perform a Markov approximation with respect to the cavity modes, as the cavity-mode reservoir has a finite bandwidth, Γ, which may only be comparable with the frequency scale Ω_0. The background-mode reservoir has an infinite bandwidth, and can therefore be treated as Markovian.

The difference between our work and that of Lewenstein *et al.* arises when we perform the quantum-mechanical average. We allow for cavity-mode correlation functions of the form

$$\begin{aligned}\langle c_k^\dagger(0)c_{k'}(0)\rangle &= N\delta(k-k')\ ,\\ \langle c_k^\dagger(0)c_{k'}^\dagger(0)\rangle &= M\delta(k+k')\ ,\end{aligned} \tag{4.5}$$

where $M=[N(N+1)]^{1/2}$, and again we have made a choice of phase for the injected squeezed vacuum which corresponds to M real. The relative phase between the coherent driving field and the squeezed vacuum can again be controlled through the phase of the coherent field ϕ_0. The expressions (4.5) will be a valid description of the cavity-mode correlation functions provided the injected squeezed field is broadband compared to the cavity linewidth.[12]

With these modifications to the statistics of the cavity-mode reservoir, we derive modified Bloch equations of the form

$$\begin{aligned}\langle \dot{S}_x\rangle =& \frac{\gamma_c}{2}\frac{\Gamma}{2}\int_0^t dt'\, e^{-\Gamma(t-t')}[\langle S_z(t)S_x(t')\rangle - i\langle S_z(t)S_y(t')\rangle + \text{c.c.}]\\ &-\gamma_c[N - M\cos(2\phi_0)]\Gamma\int_0^t dt'\, e^{-\Gamma(t-t')}\cos[\Omega_0(t-t')]\langle S_x(t')\rangle\\ &+\gamma_c M\sin(2\phi_0)\Gamma\int_0^t dt'\, e^{-\Gamma(t-t')}\cos[\Omega_0(t-t')]\langle S_y(t')\rangle\\ &-\gamma_c M\sin(2\phi_0)\Gamma\int_0^t dt'\, e^{-\Gamma(t-t')}\sin[\Omega_0(t-t')]\langle S_z(t')\rangle - \frac{\gamma_b}{2}\langle S_x\rangle\ ,\end{aligned} \tag{4.6a}$$

$$\begin{aligned}\langle \dot{S}_y\rangle =& \frac{\gamma_c}{2}\frac{\Gamma}{2}\int_0^t dt'\, e^{-\Gamma(t-t')}[i\langle S_z(t)S_x(t')\rangle + \langle S_z(t)S_y(t')\rangle + \text{c.c.}]\\ &-\gamma_c[N + M\cos(2\phi_0)]\Gamma\int_0^t dt'\, e^{-\Gamma(t-t')}\cos[\Omega_0(t-t')]\langle S_y(t')\rangle\\ &+\gamma_c M\sin(2\phi_0)\Gamma\int_0^t dt'\, e^{-\Gamma(t-t')}\cos[\Omega_0(t-t')]\langle S_x(t')\rangle\\ &+\gamma_c[N + M\cos(2\phi_0)]\Gamma\int_0^t dt'\, e^{-\Gamma(t-t')}\sin[\Omega_0(t-t')]\langle S_z(t')\rangle - \Omega_0\langle S_z\rangle - \frac{\gamma_b}{2}\langle S_y\rangle\ ,\end{aligned} \tag{4.6b}$$

$$\begin{aligned}\langle \dot{S}_z\rangle =& -\frac{\gamma_c}{2}\frac{\Gamma}{2}\int_0^t dt'\, e^{-\Gamma(t-t')}[\langle S_x(t')S_x(t)\rangle - i\langle S_x(t')S_y(t)\rangle + \text{c.c.}]\\ &-\frac{\gamma_c}{2}\frac{\Gamma}{2}\int_0^t dt'\, e^{-\Gamma(t-t')}[\langle S_y(t')S_y(t)\rangle + i\langle S_y(t')S_x(t)\rangle + \text{c.c.}]\\ &-\gamma_c[N + M\cos(2\phi_0)]\Gamma\int_0^t dt'\, e^{-\Gamma(t-t')}\sin[\Omega_0(t-t')]\langle S_y(t')\rangle\\ &-\gamma_c N\Gamma\int_0^t dt'\, e^{-\Gamma(t-t')}\{1+\cos[\Omega_0(t-t')]\}\langle S_z(t')\rangle\\ &+\gamma_c M\cos(2\phi_0)\Gamma\int_0^t dt'\, e^{-\Gamma(t-t')}\{1-\cos[\Omega_0(t-t')]\}\langle S_z(t')\rangle\\ &+\gamma_c M\sin(2\phi_0)\Gamma\int_0^t dt'\, e^{-\Gamma(t-t')}\sin[\Omega_0(t-t')]\langle S_x(t')\rangle + \Omega_0\langle S_y\rangle - \gamma_b(1+\langle S_z\rangle)\ ,\end{aligned} \tag{4.6c}$$

where S_x and S_y are defined in (2.3).

To be consistent with our first-order expansion in γ_c and γ_b, it is sufficient to calculate the correlation functions occurring in (4.6) in zeroth order (i.e., neglecting all damping). The correlation functions are thus replaced with linear combinations of one-time averages of the spin operators (evaluated at the "initial" time t'). We are again interested in the limit in which $\Omega_0 \gg \Gamma$, and so we in turn replace the $\langle S_i(t')\rangle$ appearing in the integrals with the expressions (3.6) (which relate $\langle S_i(t')\rangle$ to $\langle S_i(t)\rangle$ in zeroth order). We also require that Γ be larger than any other decay rates featuring in the dynamics, which enables us to set the integrals equal to their stationary ($t\to\infty$) values. The Bloch equations can then be written in the approximate form

$$\langle \dot{S}_x\rangle \simeq -\gamma_c[N - M\cos(2\phi_0) + \tfrac{1}{2}]\frac{\Gamma^2}{\Gamma^2+\Omega_0^2}\langle S_x\rangle + \gamma_c M\sin(2\phi_0)\langle S_y\rangle - \frac{\gamma_b}{2}\langle S_x\rangle\ , \tag{4.7a}$$

$$\langle \dot{S}_y \rangle \simeq -\gamma_c[N+M\cos(2\phi_0)+\tfrac{1}{2}]\langle S_y \rangle + \gamma_c M \sin(2\phi_0)\frac{\Gamma^2}{\Gamma^2+\Omega_0^2}\langle S_x \rangle + \gamma_c \frac{\Omega_0 \Gamma/2}{\Gamma^2+\Omega_0^2} - \Omega_0 \langle S_z \rangle - \frac{\gamma_b}{2}\langle S_y \rangle \ , \tag{4.7b}$$

$$\langle \dot{S}_z \rangle \simeq -\frac{\gamma_c}{2}\left[1+\frac{\Gamma^2}{\Gamma^2+\Omega_0^2}\right] - \gamma_c[N+M\cos(2\phi_0)+\tfrac{1}{2}]\langle S_z \rangle - \gamma_c[N-M\cos(2\phi_0)+\tfrac{1}{2}]\frac{\Gamma^2}{\Gamma^2+\Omega_0^2}\langle S_z \rangle$$
$$+\gamma_c[N-M\cos(2\phi_0)+\tfrac{1}{2}]\frac{\Gamma\Omega_0}{\Gamma^2+\Omega_0^2}\langle S_y \rangle + \gamma_c M \sin(2\phi_0)\frac{\Gamma\Omega_0}{\Gamma^2+\Omega_0^2}\langle S_x \rangle + \Omega_0\langle S_y \rangle - \gamma_b(1+\langle S_z \rangle) \ . \tag{4.7c}$$

With increasing Ω_0/Γ, many of the terms in (4.7) become very small. Neglecting these terms, we can further approximate the equations to finally produce

$$\langle \dot{S}_x \rangle \simeq \gamma_c M \sin(2\phi_0)\langle S_y \rangle - \frac{\gamma_b}{2}\langle S_x \rangle \ ,$$
$$\langle \dot{S}_y \rangle \simeq -\gamma_c[N+M\cos(2\phi_0)+\tfrac{1}{2}]\langle S_y \rangle - \Omega_0\langle S_z \rangle - \frac{\gamma_b}{2}\langle S_y \rangle \ , \tag{4.8}$$
$$\langle \dot{S}_z \rangle \simeq -\frac{\gamma_c}{2} - \gamma_c[N+M\cos(2\phi_0)+\tfrac{1}{2}]\langle S_z \rangle + \Omega_0\langle S_y \rangle - \gamma_b(1+\langle S_z \rangle) \ .$$

The most interesting choice of the phase ϕ_0 is that which gives $\cos(2\phi_0)=-1$, for in that case

$$\gamma_c[N+M\cos(2\phi_0)+\tfrac{1}{2}] = \gamma_c(N-M+\tfrac{1}{2}) \approx \frac{\gamma_c}{8N} \ , \tag{4.9}$$

for large N [see (3.14)]. Hence, with the addition of squeezing, the cavity-mode decay of *all three* components of the Bloch vector can, in principle, be strongly inhibited. The cavity spectral density provides the mechanism for the inhibition of the decay of $\langle S_x \rangle$, and for the partial (up to 33%) inhibition of the decay of $\langle S_y \rangle$ and $\langle S_z \rangle$, while the injected squeezed vacuum acts to remove the remaining decay channel for $\langle S_y \rangle$ and $\langle S_z \rangle$.

In contrast, the choice of phase $\cos(2\phi_0)=1$ leads to a dramatic enhancement of the decay of $\langle S_y \rangle$ and $\langle S_z \rangle$.

If γ_c is much larger than γ_b, then significant effects should be observable. The population decay is vitally dependent on the phase of the coherent field, varying between strongly inhibited and strongly enhanced regimes. If we assume that our observations of the behavior of the Bloch vector components can be extended to the spectrum of resonance fluorescence out the side of the cavity (Lewenstein *et al.*[11] have demonstrated that such an extension can be justified, and, indeed, our work in Sec. III also supports this), then for the choice of phase $\cos(2\phi_0)=-1$, we predict dramatic narrowing of all three peaks in the Mollow triplet. The choice of phase $\cos(2\phi_0)=1$ should result in strong broadening of the Rabi sidebands. We note that by observing the fluorescence out the side of the cavity, we obviate any complication associated with reflections of the squeezed vacuum input.

ACKNOWLEDGMENTS

I would like to thank Dr. Barry Sanders for helpful discussions and Professor Crispin Gardiner for comments on the manuscript. This work was supported by the New Zealand University Grants Committee.

[1]C. W. Gardiner, Phys. Rev. Lett. **56**, 1917 (1986).
[2]H. J. Carmichael, A. S. Lane, and D. F. Walls, Phys. Rev. Lett. **58**, 2539 (1987); J. Mod. Opt. **34**, 821 (1987).
[3]G. J. Milburn, Phys. Rev. A **34**, 4882 (1986).
[4]H. Ritsch and P. Zoller, Opt. Commun. **64**, 523 (1987); S. An, M. Sargent, and D. F. Walls, *ibid.* **67**, 373 (1988).
[5]M. A. Marte and D. F. Walls, Phys. Rev. A **37**, 1235 (1988); M. A. Marte, H. Ritsch, and D. F. Walls, Phys. Rev. Lett. **61**, 1093 (1988).
[6]A. S. Parkins and C. W. Gardiner, Phys. Rev. A **40**, 2534 (1989).
[7]C. W. Gardiner and M. J. Collett, Phys. Rev. A **31**, 3761 (1985).
[8]L.-A. Wu, H. J. Kimble, J. L. Hall, and H. Wu, Phys. Rev. Lett. **57**, 2520 (1986); L.-A. Wu, M. Xiao, and H. J. Kimble, J. Opt. Soc. Am. B **4**, 1465 (1987).
[9]A. S. Parkins and C. W. Gardiner, Phys. Rev. A **37**, 3867 (1988).
[10]H. Ritsch and P. Zoller, Phys. Rev. Lett. **61**, 1097 (1988).
[11]M. Lewenstein, T. W. Mossberg, and R. J. Glauber, Phys. Rev. Lett. **59**, 775 (1987); M. Lewenstein and T. W. Mossberg, Phys. Rev. A **37**, 2048 (1988).
[12]M. J. Collett and C. W. Gardiner, Phys. Rev. A **30**, 1386 (1984).
[13]C. W. Gardiner, *Handbook of Stochastic Methods* (Springer, Berlin, 1983).
[14]A. M. Smith and C. W. Gardiner, Phys. Rev. A **39**, 3511 (1989).
[15]C. W. Gardiner, A. S. Parkins, and M. J. Collett, J. Opt. Soc. Am. B **4**, 1683 (1987).
[16]D. J. Heinzen, J. J. Childs, J. E. Thomas, and M. S. Feld, Phys. Rev. Lett. **58**, 1320 (1987).